

## Supplementary: Strain and charge contributions to the magnetoelectric coupling in Fe<sub>3</sub>O<sub>4</sub>/PMN-PT artificial multiferroic heterostructures

Patrick Schöffmann,<sup>1, 2, \*</sup> Anirban Sarkar,<sup>1</sup> Mai Hussein Hamed,<sup>3, 4</sup> Tanvi Bhatnagar-Schöffmann,<sup>1, 2, 5</sup> Sabine Pütter,<sup>6</sup> Brian J. Kirby,<sup>7</sup> Alexander J. Grutter,<sup>7</sup> Juri Barthel,<sup>8</sup> Emmanuel Kentzinger,<sup>1</sup> Annika Stellhorn,<sup>1, 2</sup> Andrei Gloskovskii,<sup>9</sup> Martina Müller,<sup>10</sup> and Thomas Brückel<sup>1, 2</sup>

<sup>1</sup> Forschungszentrum Jülich GmbH, Jülich Centre for Neutron Science (JCNS-2) and Peter Grünberg Institut (PGI-4), JARA-FIT, 52425 Jülich, GERMANY

<sup>2</sup> RWTH Aachen, Lehrstuhl für Experimentalphysik IVc, Jülich-Aachen Research Alliance, JARA-FIT, 52074, Aachen, Germany

<sup>3</sup> Forschungszentrum Jülich GmbH, PGI-6, 52425 Jülich, GERMANY

<sup>4</sup> Faculty of Science, Helwan University, 11795 Cairo, EGYPT

<sup>5</sup> Forschungszentrum Jülich GmbH, Ernst Ruska-Centre for Microscopy and Spectroscopy with Electrons and Peter Grünberg Institute (PGI-5), 52425 Jülich, Germany

<sup>6</sup> Forschungszentrum Jülich GmbH, Jülich Centre for Neutron Science JCNS at Heinz Maier-Leibnitz Zentrum MLZ, 85748 Garching, GERMANY

<sup>7</sup> NIST Center for Neutron Research, National Institute of Standards and Technology, Gaithersburg, Maryland 20899, USA

<sup>8</sup> Forschungszentrum Jülich GmbH, Ernst Ruska-Centre for Microscopy and Spectroscopy with Electrons Materials Science and Technology (ER-C-2), 52425 Jülich, Germany

<sup>9</sup> Photon Science, Deutsches Elektronen-Synchrotron DESY, 22607 Hamburg, Germany

<sup>10</sup> Fachbereich Physik, Universität Konstanz, 78457 Konstanz, Germany

(Dated: July 20, 2022)

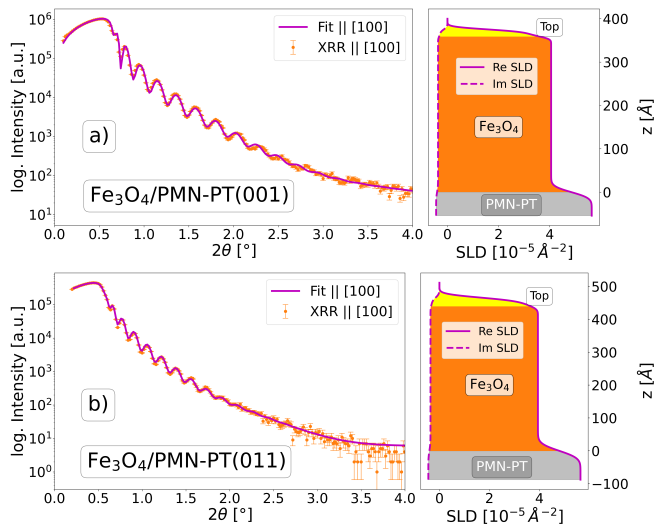


FIG. S. 1. X-ray reflectometry measurements with fit, and resulting scattering length density profile ('Re SLD' for the real part and 'Im SLD' for imaginary) for **a)** Fe<sub>3</sub>O<sub>4</sub>/PMN-PT(001) and **b)** Fe<sub>3</sub>O<sub>4</sub>/PMN-PT(011) for X-rays scattering along the [100] direction. A top layer of reduced density had to be assumed for both samples to achieve a good fit. Error bars represent square root of intensity.

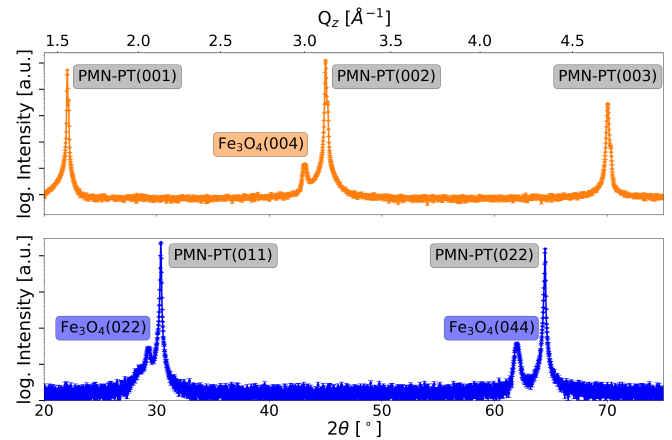


FIG. S. 2. X-ray diffraction measurement for Fe<sub>3</sub>O<sub>4</sub>/PMN-PT(001) and Fe<sub>3</sub>O<sub>4</sub>/PMN-PT(011) samples. Only peaks belonging to the substrate or Fe<sub>3</sub>O<sub>4</sub> are visible. Error bars represent square root of intensity.

of the Verwey temperature by 2.2 K in the ZFC measurement (fig. S. 4).

For the fit of the PNR data, it has to be noted that the error for the magnetisation angle is probably underestimated, especially for the top layer, as the spin-flip signal reaches background levels at around 0.035 Å<sup>-1</sup>. Since the magnetisation angle is determined by fitting the intensities of the spin-flip and non spin-flip channels, the diminished intensity of the spin-flip channel at higher Q introduces an uncertainty into the angle determination. Given that the roughness of the top layer is nearly as large as its thickness, a meaningful interpretation of the magnetisation angle is likely impossible.

Figure S. 3 shows the magnetization in presence and absence of electric field applied across the heterostructure. While the change in saturation magnetization ( $\Delta M_S/M_S$ ) is only 2% at 1 T, the coercive field ( $\Delta H_C/H_C$ ) changes by 15%. We also observe a reduction

**Fe<sub>3</sub>O<sub>4</sub>/PMN-PT(001)**

Layer	thickness [Å]	roughness [Å]
Top	16.4 <sup>+0.6</sup> <sub>-0.4</sub>	5.0 <sup>+0.2</sup> <sub>-0</sub>
Fe <sub>3</sub> O <sub>4</sub>	359 <sup>+2</sup> <sub>-2</sub>	5.0 <sup>+0.6</sup> <sub>-0</sub>
PMN-PT	-	11 <sup>+1</sup> <sub>-0.8</sub>

**Fe<sub>3</sub>O<sub>4</sub>/PMN-PT(011)**

Layer	thickness [Å]	roughness [Å]
Top	25.0 <sup>+0</sup> <sub>-0.9</sub>	10.0 <sup>+0.2</sup> <sub>-0.2</sub>
Fe <sub>3</sub> O <sub>4</sub>	441 <sup>+3</sup> <sub>-4</sub>	9.0 <sup>+0.2</sup> <sub>-0.2</sub>
PMN-PT	-	18 <sup>+3</sup> <sub>-2</sub>

TABLE S. I. Fit parameter of the XRR measurement for Fe<sub>3</sub>O<sub>4</sub>/PMN-PT(001) and Fe<sub>3</sub>O<sub>4</sub>/PMN-PT(011)

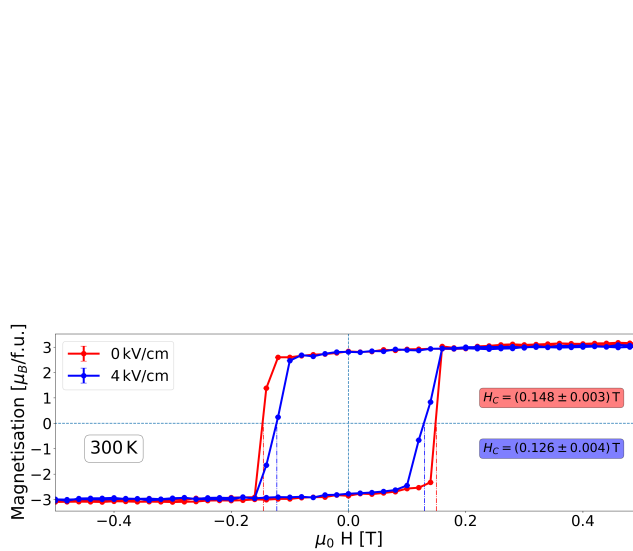


FIG. S. 3. Magnetisation hysteresis in presence and absence of 4 kV/cm electric field showing a reduction of the coercive field.

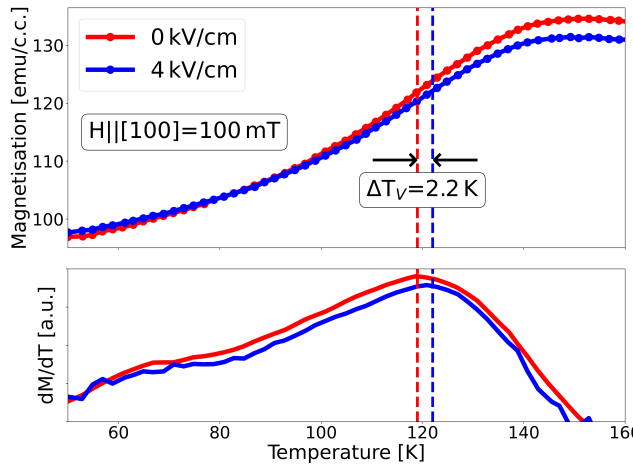


FIG. S. 4. ZFC magnetisation measurement and derivative, in presence and absence of 4 kV/cm electric field.

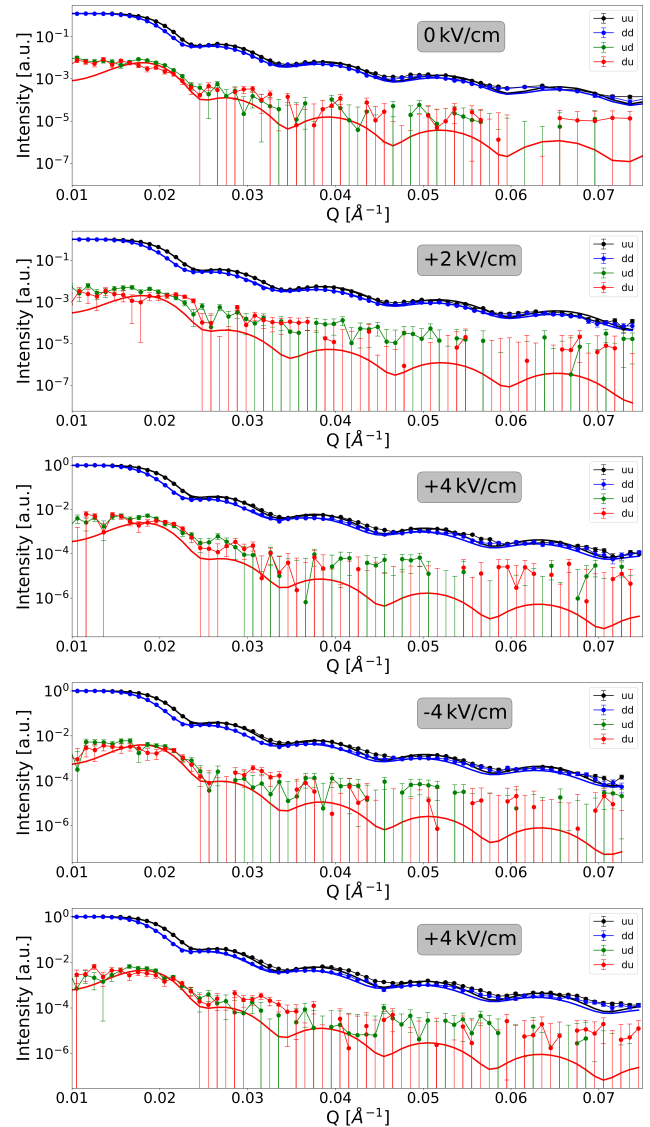


FIG. S. 5. PNR measurements with fit of Fe<sub>3</sub>O<sub>4</sub>/PMN-PT(011) with the application of voltage

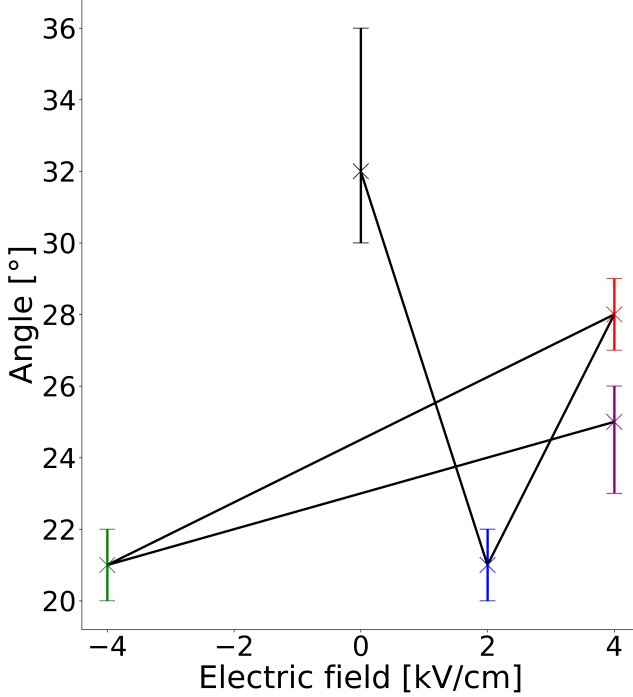


FIG. S. 6. Magnetisation angle relative to the magnetic field extracted from the fit of the PNR measurements.

Electric field [kV/cm]	Layer	Thickness [Å]	roughness [Å]	Magnetic [10 <sup>-6</sup> Å <sup>-2</sup> ]	SLD	Magnetisation angle [°]
0	Top	19.0 <sup>+0.1</sup> <sub>-0.1</sub>	5.94 <sup>+0.06</sup> <sub>-0.05</sub>	0.49 <sup>+0.01</sup> <sub>-0.01</sub>	61 <sup>+3</sup> <sub>-2</sub>	
0	Fe <sub>3</sub> O <sub>4</sub>	434.2 <sup>+1.0</sup> <sub>-0.9</sub>	10.5 <sup>+0.1</sup> <sub>-0.1</sub>	0.34 <sup>+0.01</sup> <sub>-0.01</sub>	32 <sup>+2</sup> <sub>-4</sub>	
0	Substrate	-	23.6 <sup>+0.2</sup> <sub>-0.2</sub>	-	-	
+2	Top	18.2 <sup>+0.1</sup> <sub>-0.1</sub>	8.0 <sup>+0.1</sup> <sub>-0.1</sub>	0.49 <sup>+0.01</sup> <sub>-0.01</sub>	67 <sup>+1</sup> <sub>-1</sub>	
+2	Fe <sub>3</sub> O <sub>4</sub>	447.0 <sup>+1.2</sup> <sub>-1.2</sub>	14.9 <sup>+0.1</sup> <sub>-0.1</sub>	0.41 <sup>+0.01</sup> <sub>-0.01</sub>	21 <sup>+1</sup> <sub>-1</sub>	
+2	Substrate	-	22.6 <sup>+0.2</sup> <sub>-0.1</sub>	-	-	
+4	Top	11.3 <sup>+0.1</sup> <sub>-0.1</sub>	8.9 <sup>+0.1</sup> <sub>-0.1</sub>	0.20 <sup>+0.01</sup> <sub>-0.01</sub>	-88 <sup>+1</sup> <sub>-2</sub>	
+4	Fe <sub>3</sub> O <sub>4</sub>	447.0 <sup>+1.2</sup> <sub>-1.2</sub>	8.3 <sup>+0.1</sup> <sub>-0.1</sub>	0.45 <sup>+0.01</sup> <sub>-0.01</sub>	28 <sup>+1</sup> <sub>-1</sub>	
+4	Substrate	-	23.5 <sup>+0.2</sup> <sub>-0.3</sub>	-	-	
-4	Top	8.8 <sup>+0.1</sup> <sub>-0.1</sub>	8.2 <sup>+0.1</sup> <sub>-0.1</sub>	0.49 <sup>+0.01</sup> <sub>-0.02</sub>	126 <sup>+1</sup> <sub>-2</sub>	
-4	Fe <sub>3</sub> O <sub>4</sub>	447.0 <sup>+1.2</sup> <sub>-1.2</sub>	13.3 <sup>+0.1</sup> <sub>-0.1</sub>	0.47 <sup>+0.02</sup> <sub>-0.01</sub>	21 <sup>+1</sup> <sub>-2</sub>	
-4	Substrate	-	22.7 <sup>+0.1</sup> <sub>-0.2</sub>	-	-	
+4	Top	10.1 <sup>+0.1</sup> <sub>-0.1</sub>	6.1 <sup>+0.1</sup> <sub>-0.1</sub>	0.47 <sup>+0.02</sup> <sub>-0.01</sub>	-28 <sup>+1</sup> <sub>-3</sub>	
+4	Fe <sub>3</sub> O <sub>4</sub>	447.0 <sup>+1.2</sup> <sub>-1.2</sub>	11.6 <sup>+0.1</sup> <sub>-0.1</sub>	0.48 <sup>+0.01</sup> <sub>-0.01</sub>	25 <sup>+2</sup> <sub>-1</sub>	
+4	Substrate	-	21.0 <sup>+0.2</sup> <sub>-0.1</sub>	-	-	

TABLE S. II. Fit parameter of the PNR measurements of Fe<sub>3</sub>O<sub>4</sub>/PMN-PT(011). The listed errors are the calculated 90% confidence intervals of the parameter, as given by the ReflID program.

\* E-mail: pa.schoeffmann@gmail.com